AGU PUBLICATIONS

JGR

Journal of Geophysical Research: Earth Surface

RESEARCH ARTICLE

10.1002/2014JF003170

Key Points:
- Modeling the role of psammophilous plants in sand dune dynamics
- One, two, or, first predicted here, three stable dune states
- Dunes are initially stabilized by psammophilous plants

Correspondence to:
G. Bel,
bel@bgu.ac.il

Citation:
Bel, G., and Y. Ashkenazy (2014), The effects of psammophilous plants on sand dune dynamics, *J. Geophys. Res. Earth Surf.*, *119*, doi:10.1002/2014JF003170.

Received 8 APR 2014
Accepted 9 JUL 2014
Accepted article online 12 JUL 2014

The effects of psammophilous plants on sand dune dynamics

Golan Bel[1] and Yosef Ashkenazy[1]

[1]Department of Environmental Physics, Blaustein Institutes for Desert Research, Ben-Gurion University of the Negev, Sede Boqer Campus, Israel

Abstract Mathematical models of sand dune dynamics have considered different types of sand dune cover. However, despite the important role of psammophilous plants (plants that flourish in moving-sand environments) in dune dynamics, the incorporation of their effects into mathematical models of sand dunes remains a challenging task. Here we propose a nonlinear physical model for the role of psammophilous plants in the stabilization and destabilization of sand dunes. There are two main mechanisms by which the wind affects these plants: (i) sand drift results in the burial and exposure of plants, a process that is known to result in an enhanced growth rate, and (ii) strong winds remove shoots and rhizomes and seed them in nearby locations, enhancing their growth rate. Our model describes the temporal evolution of the fractions of surface cover of regular vegetation, biogenic soil crust, and psammophilous plants. The latter reach their optimal growth under either (i) specific sand drift or (ii) specific wind power. The model exhibits complex bifurcation diagrams and dynamics, which explain observed phenomena, and it predicts new dune stabilization scenarios. Depending on the climatological conditions, it is possible to obtain one, two, or, predicted here for the first time, three stable dune states. Our model shows that the development of the different cover types depends on the precipitation rate and the wind power and that the psammophilous plants are not always the first to grow and stabilize the dunes.

1. Introduction

The dynamics of sand dunes have been studied extensively in the framework of mathematical and physical modeling [*Bagnold*, 1941; *Kok et al.*, 2012]. The complexity of their patterns and dynamics, due to physical processes at many temporal and spatial scales, poses a great challenge to modelers. Models for sand dynamics include processes at a broad range of scales: the grain scale [*Anderson and Haff*, 1988; *Forrest and Haff*, 1992; *Landry and Werner*, 1994], the scale of meters (ripples and mega ripples) [*Anderson*, 1987; *Forrest and Haff*, 1992; *Landry and Werner*, 1994; *Prigozhin*, 1999; *Yizhaq*, 2005, 2008], the scale of tens of meters (sand blowouts) [*Gares and Nordstrom*, 1995], the dune scale (scale of hundreds of meters, different dune types, such as barchan, linear, and parabolic) [*Bagnold*, 1941; *Andreotti et al.*, 2002; *Durán and Herrmann*, 2006; *de M. Luna et al.*, 2009; *Reitz et al.*, 2010; *Nield and Baas*, 2008], and mean field models of sand dune cover types (scale of kilometers) [*Yizhaq et al.*, 2007, 2013].

Sand dunes cover vast areas in arid and coastal regions ($\sim$ 10% of Earth's terrestrial surface [*Pye*, 1982; *Pye and Tsoar*, 1990; *Thomas and Wiggs*, 2008]) and, therefore, are considered to be an important component of ecosystems [*Tsoar*, 2008; *Veste et al.*, 2001; *Shanas et al.*, 2006] and climate [*Thomas et al.*, 2005; *Ashkenazy et al.*, 2012; *Otterman*, 1974; *Charney et al.*, 1975] dynamics. Dunes may be stabilized by vegetation and/or biogenic soil crust (BSC) [*Danin et al.*, 1989]; since vegetation can only exist above a certain precipitation threshold (typically $\sim$ 50 mm/year [*Tsoar*, 2005]), sand dune dynamics and activity in arid regions are affected by the precipitation rate.

Many experimental [*Bagnold*, 1941; *Fryberger and Dean*, 1979; *Pye and Tsoar*, 1990] and theoretical [*Bagnold*, 1941; *Andreotti et al.*, 2002; *Durán and Herrmann*, 2006; *de M. Luna et al.*, 2009; *Reitz et al.*, 2010; *Nield and Baas*, 2008; *Kok et al.*, 2012] works have been devoted to uncovering the mechanisms behind the geomorphology of sand dunes. Most of these models have focused on dune patterns and their corresponding scaling laws, on dune formation, and on the transition from one type of dune to another. These mathematical and physical models usually require a long integration time, therefore only enabling the simulations of relatively small dune fields. An alternative approach is to model the vegetation and BSC cover of the dunes, ignoring dune patterns and 3-D dune dynamics, and to determine dune stability (active or fixed) according to the fraction of vegetation and BSC cover; bare dunes are active, while vegetated and/or

BSC-covered dunes are fixed [*Yizhaq et al.*, 2007, 2009; *Kinast et al.*, 2013; *Yizhaq et al.*, 2013]. Such models require a relatively short computation time and have been used to explain the bistability of active and fixed dunes under similar climatic conditions. In addition, it is possible to model the development of a 2-D vegetation cover by considering the spatial effect of the wind and the diffusion of vegetation [*Yizhaq et al.*, 2013]. Both observations [*Veste et al.*, 2001] and models [*Kinast et al.*, 2013] indicate that BSC plays an important role in dune stabilization in arid regions with relatively weak winds.

The movement of windblown sand is a stress to "regular" vegetation (hereafter "vegetation"). Some species have evolved to tolerate, and even flourish in, moving-sand environments. These plants are called "psammophilous plants" [*Danin*, 1991, 1996; *Maun*, 2009]. Psammophilous plants have developed several physiological mechanisms to survive in and benefit from sand drift. Here we focus on several interactions of these plants with sand drift. The first interaction is the exposure of previously buried plants due to sand movement, which increases their photosynthesis and growth rates [*Danin*, 1991, 1996; *Maun*, 2009]. The second is the burial of plants or some of their shoots by the windblown sand; some plants that have adapted to the sandy environment respond to burial with a short-term decrease in function and growth, followed by an enhanced growth rate and function. These increases in growth rate and function are more common when the burial is temporary [*Zhang and Maun*, 1990, 1992; *Wagner*, 1964; *Martínez and Moreno-Casasola*, 1996; *Maun*, 2009]. The most likely origin of the enhanced aboveground growth is the increased root mass due to the burial [*Cheplick and Grandstaff*, 1997; *Perumal and Maun*, 2006; *Maun*, 2009]. The final interaction explicitly considered here is the removal of shoots from the plants by the wind and their burial by the sand; in some of these plants, this is the mechanism that enhances growth through the development of new plants from the wind-spread shoots [*Wallen*, 1980]. The effects of the exposure and burial (the first and second interactions mentioned above), whose rates of occurrence and efficiency are determined by the actual sand drift, will be referred to as mechanism I, and the more direct effects of the wind (the third interaction mentioned above), whose rates of occurrence and efficiency are determined by the drift potential, will be referred to as mechanism II. We note that this is an oversimplified classification of the interactions of psammophilous plants with the wind and the sand drift.

Psammophilous plants play an important role in dune stabilization. Due to their adaptation to moving-sand environments, they are the first to develop (under suitable environmental conditions) in bare and active sand dunes [*Danin*, 1996; *Maun*, 2009; *Moreno-Casasola*, 1986; *Maun*, 1998; *Martínez et al.*, 2001; *Maun*, 2009]. Once a sufficiently dense psammophilous plant cover is established, the sand movement is reduced accordingly, enabling the development of vegetation and BSC. This development further reduces the sand activity, suppressing the growth of psammophilous plants and further enhancing the growth of vegetation and BSC. This process may continue until the dunes become fixed and reach a steady state associated with the environmental conditions. Despite their important role in dune stabilization, only a few studies [*Baas and Nield*, 2010; *Eastwood et al.*, 2011] have incorporated the dynamics of psammophilous plants into mathematical models of sand dunes.

The major goal of this study is to investigate the dynamics of psammophilous plants on sand dunes, considering explicitly their interactions with vegetation and BSC. Our model neglects a continuous supply of sand and only accounts for sand drift. Therefore, we expect the model to be valid for desert dunes and coastal dunes in which the influx of sand is small. Our model differs significantly from models that consider the growth rate of psammophilous plants to depend on the overall sand flux rather than on the sand drift [*Baas and Nield*, 2010; *Eastwood et al.*, 2011]. The models that explicitly consider the geomorphology of sand dunes (such as *Baas and Nield* [2010] and *Eastwood et al.* [2011]) are able to resolve length scales of meters or less and, hence, the heterogeneous sand flux. This resolution allows the determination of preferred locations for the growth of different types of vegetation and the shape of the dunes. The mean field models, like ours, only capture processes at the scale of several dunes. Hence, the heterogeneity of the sand flux is not resolved. However, the lower resolution simplifies the dynamics significantly and enables the understanding of the large-scale effects of the interplay between different cover types. The large scale of the model also allows us to neglect the heterogeneity of the sand flux and focus on the spatially averaged sand drift. The temporal scales captured by mean field models are also larger than those captured by the more detailed models.

The model suggested below is a natural extension of the models suggested by *Yizhaq et al.* [2007] and others [*Yizhaq et al.*, 2009; *Kinast et al.*, 2013; *Yizhaq et al.*, 2009]. The model describes the development of

vegetation, BSC, and psammophilous plants on sand dunes, taking into account the effects of the wind and the precipitation. We suggest two ways to model psammophilous plants. The first approach aims to describe "mechanism I," in which the growth of the psammophilous plants is optimal under a specified sand drift. The second approach describes "mechanism II," in which psammophilous plants reach their optimal growth under a specified optimal wind power (or drift potential, defined below). The setup of the models of mechanisms I and II is different, since the drift potential, used to model the optimal growth due to mechanism II, is not affected by the actual dune cover, while the sand drift that is used to model mechanism I is strongly affected by the dune cover. Both approaches show that for some climatic conditions (a region in the drift potential and precipitation rate parameter space), the psammophilous plants act as pioneers in colonizing sand dunes, followed by vegetation and/or BSC that dominates the sand dune cover toward its stabilization. These dynamics are in agreement with the scenario suggested by *Danin* [1996] and *Maun* [2009].

2. The Model

Our model for psammophilous plants (coupled to vegetation and BSC) follows previously suggested mean field models [*Yizhaq et al.*, 2007, 2009; *Kinast et al.*, 2013] for the dynamics of vegetation and BSC cover of sand dunes. The dynamical variables in our model are the fractions of regular vegetation cover, v, BSC cover, b, and psammophilous plant cover, v_p, where v_p is a new variable added to the model described in *Kinast et al.* [2013]. The model does not account for the geomorphology of the sand dunes and adopts a very simplified view of the various interactions involved in dune dynamics (see, for example, the much more complicated models considered in *Baas and Nield* [2010], *Eastwood et al.* [2011], and references therein). However, its simplicity and the relatively small number of variables and parameters offer an excellent opportunity to understand different mechanisms of large-scale dune stabilization and activation by varying climatic conditions.

The effects considered in the previous models [*Yizhaq et al.*, 2007, 2009; *Kinast et al.*, 2013], as well as in this model, may be divided into three categories: effects that are not related to the wind, effects that are directly related to the wind, and effects that are indirectly related to the wind (representing effects of sand drift). The effects that are not related to the wind include the growth and mortality of the different cover types. We assume a logistic-type growth [*Baudena et al.*, 2007]. The logistic growth is a simple mathematical formulation of the fact that a small population growth rate is independent of the population density, while at higher population density, the growth rate diminishes as the population density approaches the carrying capacity of the ecosystem. The natural growth rate, $\alpha_j(p)$ (j stands for the cover type, either b, v, or v_p), depends on the precipitation rate, p; for simplicity and consistency with previous works, we adopt the form of [*Yizhaq et al.*, 2007, 2009; *Kinast et al.*, 2013; *Yizhaq et al.*, 2013]

$$\alpha_j(p) \equiv \alpha\_\max_j \left(1 - \exp\left(-\frac{p - p\_\min_j}{c_j}\right)\right) \qquad j \in \{v, v_p, b\}, \tag{1}$$

where $\alpha\_\max_j$ is the maximal growth rate of the jth cover type. This maximal growth rate is achieved when the precipitation rate, p, is high enough not to be a growth-limiting factor and when the other climatic conditions are optimal. The parameter characterizing how sharply the growth rate saturates with an increasing precipitation rate is c_j. In addition, we consider the spontaneous growth of the cover types (growth occurring even in bare dunes) due to effects not modeled here, such as the soil seed bank, underground roots, and seed dispersal by the wind and animals. These effects are characterized by spontaneous growth rates, η_j. The wind-independent mortality is accounted for by an effective mortality rate for each cover type, μ_j.

In modeling the direct and indirect effects of the wind, we use the wind drift potential, D_p, as a measure of the wind power [*Fryberger and Dean*, 1979]; D_p is linearly proportional to the sand drift. The wind drift potential is defined as

$$D_p \equiv \langle U^2 \left(U - U_t\right)\rangle, \tag{2}$$

where U is the wind speed (at 10 m height above the ground) measured in knots (1 knot = 0.514 m/s), $U_t = 12$ knots is the threshold wind speed necessary for sand transport, and the $\langle\cdot\rangle$ denotes a time average. When the wind speed, U, is measured in knots, D_p is measured in vector units, VU $\equiv$ knot^3. This relation is based on the Lettau equations [*Fryberger and Dean*, 1979]. D_p provides only the potential value of sand drift; in the case of unidirectional wind, it coincides with the resultant wind drift potential (RDP), which

also takes into account the wind direction. Here we assume that the winds are unidirectional and use D_p instead of RDP.

Two wind effects are considered in our model. The first is the direct damage or mortality by the wind, which is proportional to the square of the wind speed (which is proportional to the wind stress) [*Frederiksen et al.*, 2006]. For simplicity, and in order to minimize the number of the parameters in the model, we assume that the direct damage by the wind is proportional to $D_p^{2/3}$ [*Fryrear and Downes*, 1975], which is a good approximation of the wind stress. The second effect is the movement of windblown sand—that is, sand drift. The sand drift is equal to the drift potential multiplied by the amount of sand multiplied by a function of the fraction of vegetation covers, $g(v, v_p)$, which accounts for the reduction of sand drift by the vegetation [*Lee and Soliman*, 1977; *Wolfe and Nickling*, 1993]. The sand drift shading function, $g(v, v_p)$, is assumed to be a steplike function that, above some critical value of the vegetation cover, v_c, drops to zero, while for values of the vegetation cover much lower than v_c, it obtains its maximal value, 1 [*Lee and Soliman*, 1977]. For simplicity, it is assumed that $g(v, v_p)$ is a function of the difference between the actual fraction of vegetation cover, $v + v_p$, and the critical value v_c. In the previous models [*Yizhaq et al.*, 2007, 2009; *Kinast et al.*, 2013; *Yizhaq et al.*, 2013], the sand drift was considered as a damaging effect, increasing the mortality of regular vegetation and BSC due to root exposure and aboveground biomass burial by the sand.

Here we focus on the role of psammophilous plants, considering their cover fraction, v_p, as a dynamical variable with a unique interaction with the sand drift. The psammophilous plants reach their maximal growth rate under optimal sand drift [*Danin*, 1996; *Maun*, 2009, 1998; *Martínez et al.*, 2001], providing them with the necessary rate of sand cover and/or exposure and branch/leaf seeding (the two mechanisms described in section 1). These unusual optimal conditions yield different dynamics of psammophilous plants. These dynamics, when coupled with the dynamics of the regular vegetation and BSC, lead to interesting and complex bifurcation diagrams (steady states) of the sand dunes and their cover types. The complete set of equations describing the dynamics of the sand dune cover types is

$$\partial_t v = \alpha_v(p)\left(v + \eta_v\right) s - \gamma_v D_p^{2/3} v - \epsilon_v v D - \mu_v v, \tag{3}$$

$$\partial_t v_p = \alpha_{v_p}(p)\left(v_p + \eta_{v_p}\right) s - \gamma_{v_p} D_p^{2/3} v_p - \epsilon_{v_p} v_p f_i\left(D_p, v, b, v_p\right) - \mu_{v_p} v_p, \tag{4}$$

$$\partial_t b = \alpha_b(p)\left(b + \eta_b\right) s - \epsilon_b b D - \mu_b b. \tag{5}$$

We introduce the following notations: s is the fraction of bare sand

$$s \equiv 1 - v - v_p - b. \tag{6}$$

The sand drift, D, is defined as

$$D \equiv D_p \times g\left(v + v_p - v_c\right) \times s. \tag{7}$$

The sand drift shading function is defined as

$$g(x) \equiv \begin{cases} 1 & x < -1/d \\ 0.5\,(1 - xd) & -1/d < x < 1/d \\ 0 & x > 1/d \end{cases} \tag{8}$$

where the parameter d determines the sharpness of the transition from total sand drift shading to its absence.

The effect of sand drift on psammophilous plants is different from its effect on the other types of sand cover. Here we consider two different options of modeling this unique interaction of psammophilous plants with sand drift, mechanisms I and II, which were explained above. These two mechanisms are modeled using different forms of the function $f_i\left(D_p, v, b, v_p\right)$.

In the first approach (mechanism I), only the sand drift is assumed to affect the dynamics of v_p. Therefore, the mortality depends only on the sand drift, $f_I\left(D_p, v, b, v_p\right) = Q(D)$. $Q(D)$ obtains its minimal value, $Q\left(D_{\text{opt}}\right) = 0$, for $D = D_{\text{opt}}$. Away from the optimal sand drift conditions, $Q(D)$ is larger than zero and hence introduces a

Table 1. Model Parameters[a]

Symbol	Meaning	Value
α_max_v	Maximal growth rate of v	0.15/year
p_min_v	Minimal rainfall needed for v growth	50 mm/year
c_v	Saturation coefficient of the v growth rate	100 mm/year
η_v	Spontaneous growth rate of v	0.2 (dimensionless)
μ_v	Non-Aeolian mortality rate of v	0
γ_v	v vulnerability to wind shear stress	0.0008 $VU^{3/2}$/year
ϵ_v	Sand transport-induced mortality parameter of v	0.001/VU/year
α_max_b	Maximal growth rate of BSC	0.015/year
p_min_b	Minimal rainfall needed for BSC growth	20 mm/year
c_b	Saturation coefficient of the BSC growth rate	50 mm/year
η_b	Spontaneous growth rate of BSC	0.15 (dimensionless)
ϵ_b	Sand transport-induced mortality parameter of BSC	0.0001/VU/year
$\alpha\_max_{v_p}$	Maximal growth rate of v_p	0.15/year
$p\_min_{v_p}$	Minimal rainfall needed for v_p growth	50 mm/year
c_{v_p}	Saturation coefficient of the v_p growth rate	100 mm/year
η_{v_p}	Spontaneous growth rate of v_p	0.2 (dimensionless)
γ_{v_p}	v_p vulnerability to wind shear stress	0.0006 $VU^{3/2}$/year
σ	Range of optimal sand drift or drift potential	100 VU
v_c	Critical vegetation cover	0.3 (dimensionless)
d	Steepness of sand drift shading	$15/2.35 \approx 6.38$

[a] v stands for regular vegetation, and v_p stands for psammophilous vegetation.

mortality term due to the nonoptimal sand drift conditions. This form of the function $Q(D)$ reflects the fact that the maximal growth rate, $\alpha\_max_{v_p}$, is assumed to be under optimal sand drift conditions. We thus use the following form of $Q(D)$

$$Q(D) \equiv \begin{cases} \frac{1}{\sigma^2}\left(D - D_{\text{opt}}\right)^2 & \left|D - D_{\text{opt}}\right| < \sigma \\ 1 & \left|D - D_{\text{opt}}\right| > \sigma \end{cases} \tag{9}$$

This choice of the function reflects the behavior described above. Other choices of the function $Q(D)$ (such as $1 - \exp\left(\left(D - D_{\text{opt}}\right)^2/\sigma^2\right)$) yield similar results. Therefore, we focus on this choice. It is important to note that this form of the function ensures that v_p cannot be much larger than v_c ($v_p >> v_c$ would lead to significantly reduced sand drift and, therefore, to sand drift that is much lower than is optimal).

The second approach to model the enhanced growth of psammophilous plants under sand drift conditions (mechanism II) is simpler and assumes that the optimal growth conditions are achieved under an optimal wind drift potential rather than under optimal sand drift conditions. Therefore, we assume that $f_{II}\left(D_p, v, b, v_p\right) = D \times R\left(D_p\right)$, where

$$R\left(D_p\right) \equiv 1 - \rho \exp\left(\frac{\left(D_p - D_{p,\text{opt}}\right)^2}{2\sigma^2}\right). \tag{10}$$

The parameter $\rho > 1$ and is set to ensure that the maximal value of v_p will not exceed v_c. Note that when $(D_p - D_{p,\text{opt}})^2 \gg 2\sigma^2$, this vegetation growth term turns into an indirect mortality term, similar to the interaction of regular vegetation with the sand drift.

Below, we refer to the different approaches as models I and II, respectively (corresponding to mechanisms I and II for the enhanced net growth of psammophilous plants). For consistency with previous studies [*Yizhaq et al.*, 2007, 2009; *Kinast et al.*, 2013], we use the parameters listed in Table 1 (for a discussion of the choice of the value of d, see *Yizhaq et al.* [2009]). In model I, $\epsilon_{v_p} = 0.2$/year, $\mu_{v_p} = 0$, and $D_{\text{opt}} = 300$ VU, while in model II, $\epsilon_{v_p} = \epsilon_v = 0.001$/VU/year, $\mu_{v_p} = 1.2$/year, $D_{p,\text{opt}} = 300$ VU, and $\rho = 5.0072$. In what follows, the drift potential, D_p, will be measured in units of VU, the precipitation rate, p, in units of mm/year, and the mortality rate of the BSC, μ_b, in units of 1/year. Time is measured in years. Justification regarding the choice of the parameters and the model setup can be obtained from *Yizhaq et al.* [2007, 2009] and *Kinast et al.* [2013].

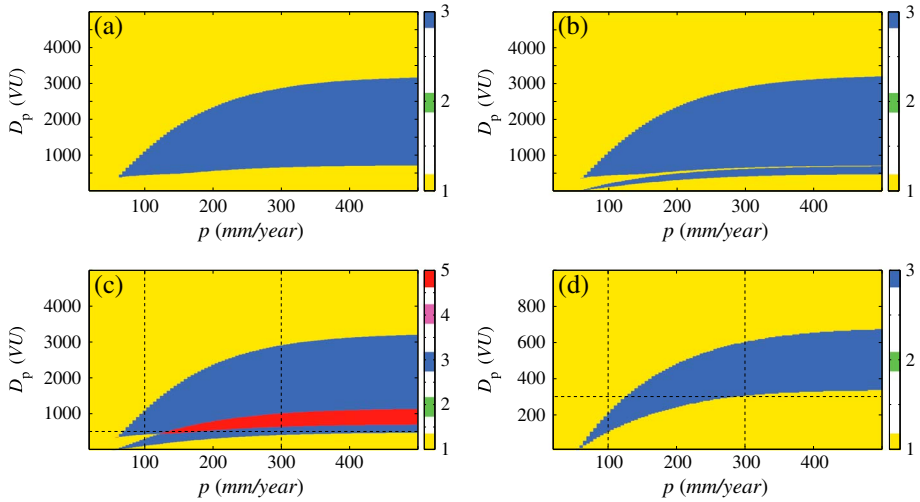

Figure 1. Maps of the number of solutions as a function of the precipitation rate, p, and the wind drift potential D_p. (a–c) Model I with BSC mortality rates $\mu_b = 0.001$, 0.006, and 0.01 (measured in units of 1/year), respectively. (d) Model II and BSC mortality rate $\mu_b = 0.006$/year.

Note that for simplicity, we do not include direct competition terms between the different model variables, unlike *Kinast et al.* [2013]. Below, we present results for different values of D_p, p, and μ_b.

3. Results

The two main climatic factors that affect sand dune dynamics are the wind conditions, which are characterized by the drift potential, D_p, and the precipitation rate, p. We first study the number of physical solutions ($0 < v, v_p, b < 1$) for given climatic conditions (D_p and p). We find that the number of solutions strongly depends on the maximal value of the BSC cover, which is determined by the BSC mortality rate, μ_b, and the other parameters. In Figure 1, we show maps of the total number of physical solutions (both stable and unstable) for different values of p and D_p. Figures 1a–1c correspond to model I and BSC mortality rates $\mu_b = 0.001$/year, 0.006/year, and 0.01/year, respectively. Figure 1a corresponds to a small value of the BSC mortality rate, $\mu_b = 0.001$/year, and it shows the existence of a typical bistability region (the region with three solutions, two of which are stable and one is unstable). Figure 1b corresponds to a higher value of the BSC mortality rate, $\mu_b = 0.006$/year, for which we have two regions of bistability. Figure 1c corresponds to an even higher value of the BSC mortality rate, $\mu_b = 0.01$/year, for which we obtain two regions of bistability and, in addition, a region of tristability (the total number of steady states is five). Figure 1d corresponds to model II with $\mu_b = 0.006$/year. It shows the existence of a bistability range. For much smaller BSC mortality rates, model II does not show a bistability region; higher values of μ_b change the location (in the parameter space) of the bistability region but do not result in a qualitatively different bifurcation diagram.

Figure 1 shows that the approaches adopted in models I and II result in different numbers of physical steady state solutions. In model I, for all three values of μ_b considered here, we have at least one range with three physical solutions (as shown in Figure 1). Two of the three solutions are stable and one is unstable. As we increase the mortality rate of the BSC (see Figure 1b), and thereby reduce the maximal value of b, a second region of bistability appears. A further increase of μ_b results in an overlap of the two bistability regions and, therefore, in a range of tristability in which we have five physical solutions (three stable solutions and two unstable ones, see Figure 1c). The two bistability regions are due to the different actions of the sand drift shading on the regular and the psammophilous plants. Small values of μ_b allow high values of b, and therefore, the only possible bistability is due to either low or high values of v_p, which, by shading, reduce the sand drift even for high values of D_p. It is important to note that in this case, one of the states corresponds to active dunes, while the other corresponds to marginally stable dunes. The psammophilous plants can never cover the dunes to the extent to which there is no sand drift because they cannot survive away from the optimal sand drift, D_{opt}. The mortality due to sand drift is reduced by the growth of a

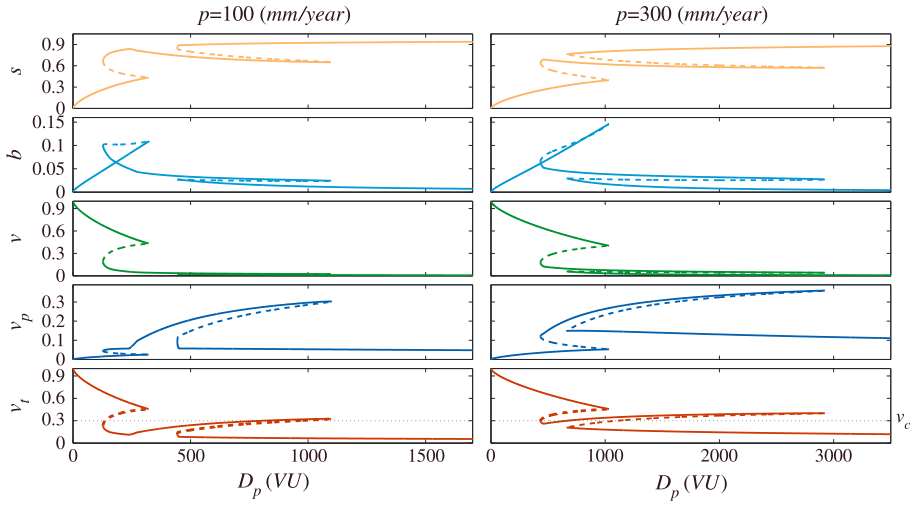

Figure 2. Bifurcation diagrams versus the drift potential, D_p, as predicted by model I along the vertical dashed lines indicated in Figure 1c. (left) Precipitation rate, $p = 100$ mm/year; (right) $p = 300$ mm/year. The rows (from top to bottom) correspond to the fractions of uncovered sand, s, BSC cover, b, psammophilous plant cover, v_p, regular vegetation cover, v, and the total sand drift shading vegetation, $v_t \equiv v_p + v$ (the dotted line marks the critical value of the vegetation cover for sand drift shading, v_c). The solid (dashed) lines correspond to stable (unstable) states. The BSC mortality rate is $\mu_b = 0.01$/year.

low value of v_p toward the critical cover, v_c, thereby accelerating this growth. However, once v_p is larger than the critical value, the sand drift sharply decreases and the mortality of the psammophilous plants increases significantly, which in turn, reduces v_p. The combination of these two actions results in a stable state at which $v_t \approx v_c$. For higher values of μ_b, the bistability of active and stable dunes, due to sand drift shading by regular plants [*Kinast et al.*, 2013], appears and creates the second range of bistability for lower values of D_p. Further increasing the BSC mortality rate results in an overlap of the two bistability ranges and, therefore, in a range of tristability. In model II, there is, at most, one region of bistability, as shown in Figure 1d. For the parameters explored here, we could not identify two distinct mechanisms of bistability. For much smaller values of μ_b, there is no bistability range, and for all values of p and D_p, there is only one physical solution. For larger values of μ_b, the bifurcation diagram is qualitatively the same as the one presented in Figure 1d. Similar behavior is obtained when considering only vegetation [*Yizhaq et al.*, 2009] and when considering BSC in addition to regular vegetation [*Kinast et al.*, 2013].

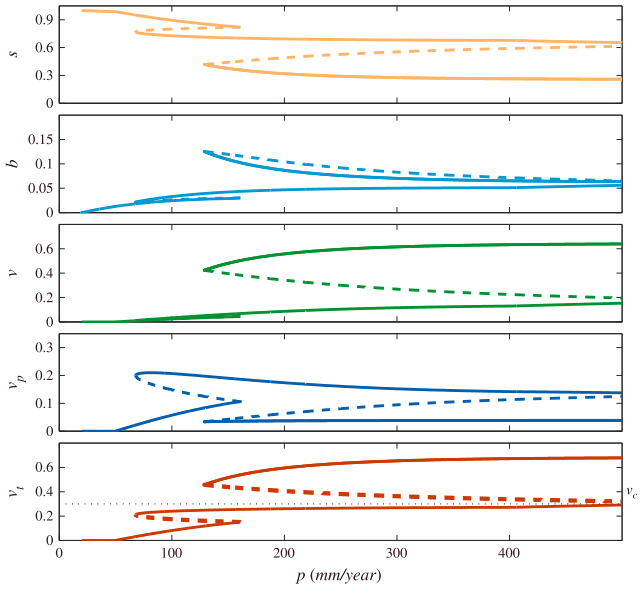

Figure 3. Bifurcation diagrams versus the precipitation rate, p, as predicted by model I along the horizontal dashed line of Figure 1c. The different rows correspond to the cover type fractions as in Figure 2. The drift potential was set to $D_p = 500$ VU, to capture all the solution branches. The BSC mortality rate was set to $\mu_b = 0.01$/year.

To better understand the complex steady state phase space, we present in Figure 2 the bifurcation diagrams, as predicted by model I, against the drift potential. These bifurcation diagrams show cross sections along the vertical dashed lines in Figure 1c. The two columns correspond to two values of the precipitation rate. The different rows correspond to the

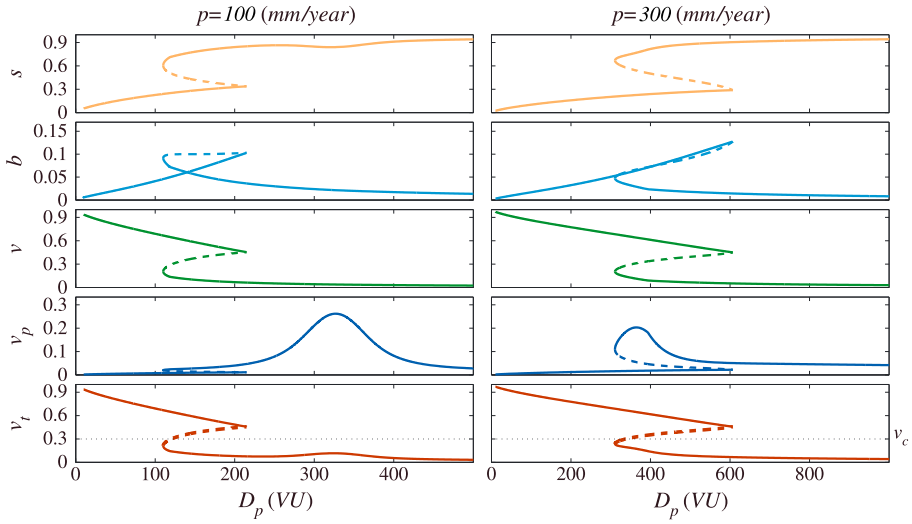

Figure 4. Bifurcation diagrams as predicted by model II along the vertical dashed lines of Figure 1d. The bifurcation parameter is the drift potential, D_p. The different rows correspond to the cover type fractions, as in Figure 2. (left) Precipitation rate, $p = 100$ mm/year; (right) precipitation rate, $p = 300$ mm/year.

different cover type fractions. We also present the following: (i) the total vegetation cover ($v + v_p$), which determines the stability of the dunes and (ii) the fraction of exposed sand. Obviously, these two variables may be extracted from v, b, and v_p and are only shown for clarity.

For the higher value of the precipitation rate, $p = 300$ mm/year, there are two D_p ranges of a single stable state (for low and high values of D_p). In addition, there are two ranges of bistability—one in which the dunes may be exposed or densely covered and a second range in which the dunes may be exposed or partially covered ($v_t \sim v_c$). In between the two bistability ranges, there is a range of D_p for which we have tristability. Namely, the dunes may be exposed, densely covered, or partially covered. For the smaller precipitation rate, $p = 100$ mm/year, the tristability range disappears. The value of the BSC mortality was set equal to the value used in Figure 1c to capture the more complicated bifurcation diagrams.

To complete the picture of the bifurcation diagrams, as predicted by model I, we show in Figure 3 the bifurcation diagrams against the precipitation rate for a fixed value of the drift potential ($D_p = 500$ VU, set to ensure that all of the five physical solutions are captured). These diagrams correspond to a cross section along the dashed horizontal line in Figure 1c. In these diagrams, one can see the onset of bistability, followed by the onset of tristability, which disappears as the precipitation rate increases.

Figure 4 depicts the bifurcation diagrams versus the drift potential, as predicted by model II, for precipitation rates of $p = 100$ mm/year and $p = 300$ mm/year. The diagrams are taken along cross sections corresponding to the dashed vertical lines in Figure 1d. For both values of the precipitation rate, there is only one bistability range. However, its width, shape, and location (in the parameter space) are affected by the value of p. A significant difference between model II and model I is the lack in the former of a steady state corresponding to partially covered dunes ($v_t \sim v_c$).

Bifurcation diagrams versus the precipitation rate as predicted by model II are presented in Figure 5. The drift potential was set to the optimal value for psammophilous plants according to this model, $D_p = 300$ mm/year (corresponding to the horizontal dashed line in Figure 1d). In these diagrams, one can see the onset of bistability and its disappearance as the precipitation rate increases.

The bifurcation diagrams alone do not elucidate all the information provided by the models. The dynamics are of relevance and importance to understanding the role of psammophilous plants in sand dune dynamics. We begin exploring the dynamics predicted by the models by investigating the steady state reached from different initial conditions. In Figure 6, we show the steady states reached using model I. Figures 6a–6d correspond to the initial conditions of bare sand dunes ($v(t = 0) = b(t = 0) = v_p(t = 0) = 0$), vegetation-covered sand dunes ($v(t = 0) = 1; b(t = 0) = v_p(t = 0) = 0$), BSC-covered sand

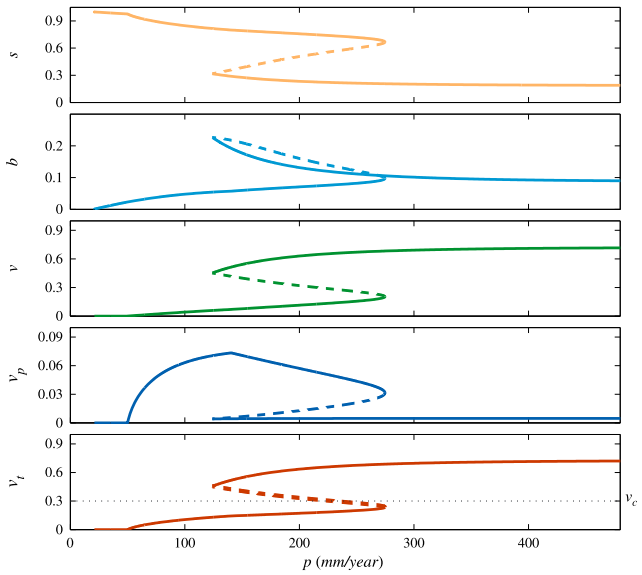

Figure 5. Bifurcation diagrams as predicted by model II. The bifurcation parameter is the precipitation rate, p. The different rows correspond to the cover type fractions. The drift potential was set to $D_p = 300$ VU.

dunes ($v(t = 0) = 0; b(t = 0) = 1; v_p(t = 0) = 0$) and psammophilous-plant-covered sand dunes ($v(t = 0) = b(t = 0) = 0; v_p(t = 0) = 1$), respectively. The different rows correspond to the cover type fractions. Here again, for convenience, we show the exposed sand fraction.

The different initial conditions result in different steady state maps. For all initial conditions, we find that for a low drift potential and a not-too-low precipitation rate (the lowest part of the panels of the first row in Figure 6), the vegetation cover dominates and stabilizes the sand dunes. For the full-vegetation-cover initial condition, the vegetation remains dominant, even at higher values of the drift potential (see Figure 6b). For all initial conditions and climatic conditions, except for a small regime of intermediate drift potential and low precipitation, the fraction of BSC cover is relatively small. The steady state with a maximal fraction of BSC cover is obtained for intermediate values of the drift potential and a not-too-small precipitation rate for an initial condition of full-vegetation cover (see Figure 6b).

The psammophilous plant cover fraction is significant for intermediate and high values of the drift potential for all initial conditions except for the full-vegetation-cover initial condition for which v_p only dominates at

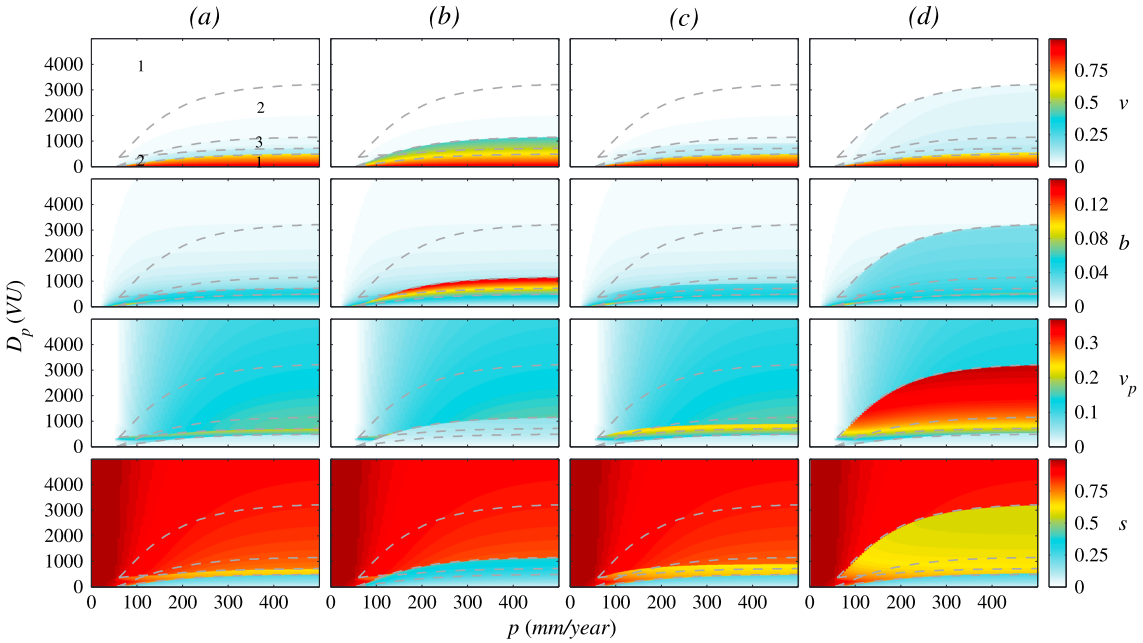

Figure 6. The steady states corresponding to different initial conditions as predicted by model I as a function of p and D_p. (a) The bare-dune initial condition, $v(t = 0) = b(t = 0) = v_p(t = 0) = 0$. (b) The vegetation-covered-dune initial condition, $v(t = 0) = 1; b(t = 0) = v_p(t = 0) = 0$. (c) The crust-covered-dune initial condition, $v(t = 0) = 0; b(t = 0) = 1; v_p(t = 0) = 0$. (d) The psammophilous plant-covered-dune initial condition, $v(t = 0) = b(t = 0) = 0; v_p(t = 0) = 1$. The different rows correspond to the different cover type fractions as indicated. The dashed lines mark the edges of the multistability regimes, namely, the crossing lines between regions with different numbers of physical solutions as shown in Figure 1c. The numbers in the top left indicate the number of stable physical solutions in each region.

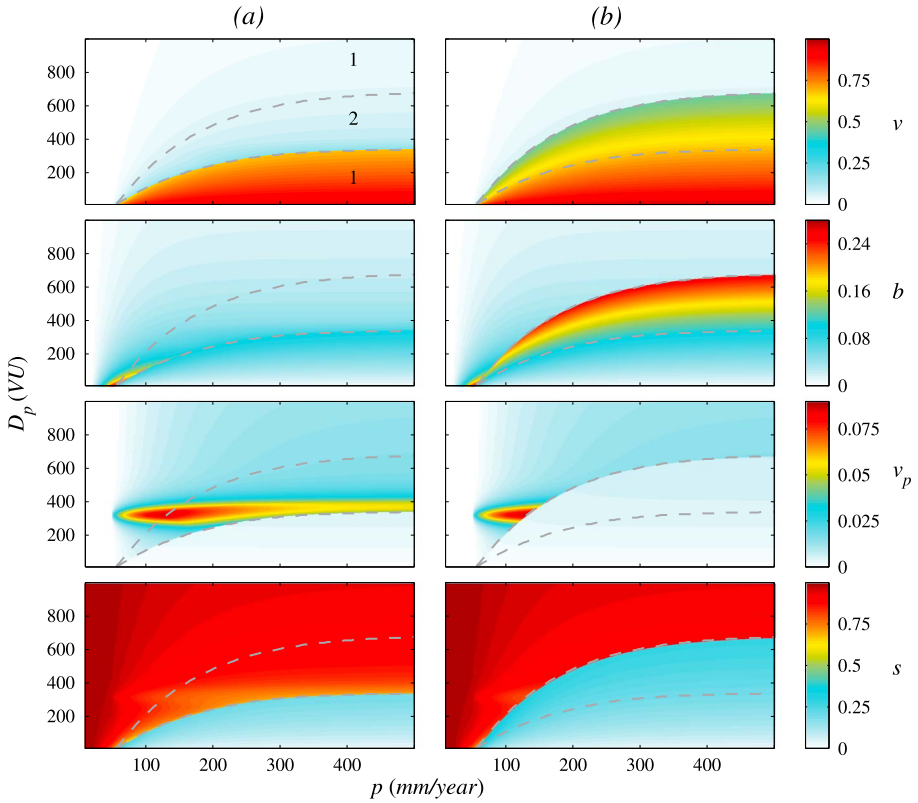

Figure 7. The steady states corresponding to different initial conditions as a function of p and D_p, as predicted by model II. (a) The bare-dune initial condition, $v(t = 0) = b(t = 0) = v_p(t = 0) = 0$, and (b) the full-vegetation-covered initial condition, $v(t = 0) = 1; b(t = 0) = v_p(t = 0) = 0$. The different rows correspond to the different cover type fractions as indicated. The dashed lines mark the edges of the bistability regime as shown in Figure 1d. The numbers in the top left indicate the number of stable solutions in each region.

high values of the drift potential. The maximal value of v_p is obtained for the $v_p = 1$ initial condition. These results suggest that the basin of attraction of the steady state solution with $v_p \sim v_c$ is relatively small if there is a stable state with a high value of v.

The bottom row in Figure 6 shows that for a bare dune initial condition, stabilization of the dunes is only possible at a high enough precipitation rate and a low drift potential. For a small range of intermediate drift potential, the steady state is partially covered dunes, namely, $v_t \sim v_c$. For the $v = 1$ initial condition, we found that the dunes remain stabilized for a high enough precipitation rate and an intermediate or weak drift potential. Note that for this initial condition, the partially covered dune steady state does not appear (for any climatic condition). For the $b = 1$ initial condition, the steady state map is very similar to the map obtained for the bare dune initial condition. However, the region of partially covered dunes in steady state is larger and extends to higher values of the drift potential. For the $v_p = 1$ initial condition, the steady state map shows a large region of partially covered dunes in steady state. Here this region extends to very high values of the drift potential.

Figure 7 shows the steady states of model II reached by different initial conditions. Figure 7a corresponds to the bare-dune initial condition, and Figure 7b corresponds to the full-vegetation-cover initial condition. Initial conditions of full psammophilous plant and BSC cover resulted in the same steady state as the bare-dune initial condition. These results suggest that the basins of attraction of the states in the bistability regime are determined by the value of v and are less sensitive to the values of b and v_p in this model. Similarly to model I, we find that in model II, for all initial conditions, a low drift potential, and a not-too-low precipitation rate, the vegetation cover dominates and stabilizes the sand dunes. For the full-vegetation-cover initial condition, the vegetation remains dominant, even at higher values of the drift potential (see Figure 7b). Note that for the parameters used here, the values of the drift potential are significantly lower than the values predicted by model I; it is possible to extend these regions by choosing a larger

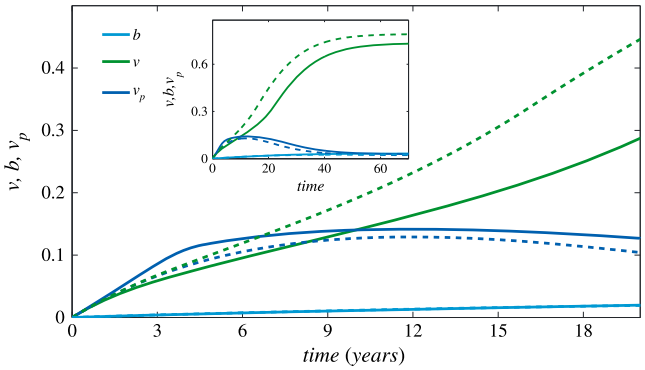

Figure 8. Time evolution of the cover type fractions as predicted by model I. The precipitation rate was set to $p = 300$ mm/year. The dashed lines correspond to drift potential, $D_p = 200$ VU, and the solid lines correspond to $D_p = 300$ VU. The solid lines show dynamics in which the psammophilous plants initially dominate and, later on, the normal vegetation dominates. The dashed lines show an evolution in which the psammophilous plants and the normal vegetation grow equally at first, and, later on, the normal vegetation dominates.

maximal growth rate, $\alpha_{v,\max}$. For the bare-dune initial condition, the fraction of BSC cover is small in all climatic conditions except for a small region of low precipitation and drift potential at which only the BSC can grow. For the $v = 1$ initial condition and not-too-low values of the drift potential, the values of b are significant; yet, these values are smaller than the values of v under the same climatic conditions. We see that for the parameters used in model II, the maximal values of v_p are significantly smaller than those obtained for model I. The only regions with significant values of v_p in steady state are around $D_{p,\mathrm{opt}}$. For the bare-dune initial condition, the region extends to high precipitation rates, while for the full-vegetation-cover initial condition, this region is truncated at low precipitation rates. The bottom row of Figure 7 shows that the stability map of the sand dunes is similar to that obtained when the psammophilous plants are neglected and only the vegetation and BSC are considered as dynamical variables.

A common paradigm for the stabilization of sand dunes under high sand drift is that the psammophilous plants act as pioneers [*Danin*, 1996; *Li et al.*, 1992, 1997; *Zhang et al.*, 2005; *Maun*, 2009]. Due to their ability to flourish under significant sand drift, they are the first to colonize bare dunes. Their growth reduces the sand drift by wind shading and enables the growth of regular vegetation, eventually resulting in stabilized dunes on which the fraction of vegetation cover dominates. In order to test whether our models are capable of reproducing this paradigm, we investigate the temporal dynamics. In Figure 8, we show the values of v, b, and v_p versus the time for the bare-dune initial condition. The precipitation rate was set to $p = 300$ mm/year. The dashed lines correspond to $D_p = 200$ VU, and the solid lines correspond to $D_p = 300$ VU. Our results show that under some climatic conditions, the dynamics follow the paradigm (the solid lines), while under other climatic conditions, the initial growth of the vegetation is identical to the initial growth of the psammophilous plants (the dashed lines). The results presented in Figure 8 were calculated using model I. For the same climatic conditions, model II yields qualitatively the same results.

4. Summary and Discussion

We have studied the effect of psammophilous plants on the dynamics of sand dunes using a simple mean field model for sand dune cover dynamics (vegetation, BSC, and psammophilous plants). Two main mechanisms of interaction of the psammophilous plants with the wind and the sand drift were modeled separately. Root exposure and the covering of branches/leaves by the sand drift enhance the net growth of psammophilous plants and result in maximal growth under optimal sand drift conditions (model I). Branches and leaves removed by the wind and buried by the sand develop new plants and increase the growth rate of psammophilous plants under an optimal wind drift potential (model II). These two approaches resulted in qualitatively different steady states and dynamics; the sand drift optimal growth model (model I) shows a richer steady state map, with up to three stable dune states (extensive sand cover, moderate sand cover, and small sand cover), while the wind drift potential optimal growth rate (model II) shows up to two stable dune states (extensive and small sand cover).

The model predicts up to three different stable steady states. The obvious stable steady state corresponds to bare-active dunes. This state is found for a low precipitation rate and/or high drift potential. Under these climatic conditions, the mortality rate of the vegetation is larger than the growth rate, and therefore, the bare dunes remain stable. The second stable steady state observed corresponds to dunes that are sufficiently vegetated to reduce the sand drift significantly, thereby decreasing the mortality rate of the vegetation and

stabilizing the covered dunes. The vegetation-covered dunes are observed under a sufficiently high precipitation rate. The third stable steady state corresponds to partially covered dunes. In this state, the dune cover is dominated by psammophilous plants. This state is observed for a high drift potential and precipitation rate, high enough to allow the development of significant psammophilous plant cover. The stability of this state is obtained due to the effect of the sand drift on the growth of the psammophilous plants. A cover fraction of the psammophilous plants, v_p, which is below the critical cover for eliminating the sand drift, v_c, can grow further. Once it significantly exceeds v_c, the sand drift is significantly reduced and the psammophilous plant mortality rate grows. This interplay results in a stable steady state in which $v_p \sim v_c$.

The steady states mentioned above are not exclusive, and either a bistability or tristability of the states is found in some ranges of climatic conditions. The underlying mechanism of the bistability of fixed vegetated dunes with bare-active dunes was discussed in previous papers [*Yizhaq et al.*, 2007, 2009; *Kinast et al.*, 2013] and can be summarized as follows. The origin of the bistability is the function $g(v_c - v_t)$ that represents the dependence of erosion and deposition processes (sand drift) on the vegetation cover. Starting from a vegetated dune, it is possible to decrease the vegetation cover by increasing the wind power (or decreasing precipitation). The dune will gradually become less vegetated and more active until the vegetation cover decreases to the critical vegetation cover, at which point the mortality rate, due to sand drift, increases significantly. This enhanced mortality will further reduce the vegetation cover and result in an active, almost bare, dune. It is possible to stabilize an active dune by increasing the vegetation and BSC cover by either decreasing the wind power or increasing the precipitation rate. However, as long as the dune vegetation cover is below the critical vegetation cover, the mortality term associated with sand drift will be significant. For this reason, the dune will be stabilized only under very small wind power and a sufficiently high precipitation rate. Hence, it is possible to find both active (bare) and fixed (vegetated) dunes for a range of wind power and precipitation rates.

The effects of sand drift on psammophilous plants introduce an additional mechanism for multistability. Starting from a dune partially covered by psammophilous plants ($v_p \sim v_c$ corresponding to optimal sand drift), it is possible to decrease their cover by increasing the wind power (or decreasing precipitation). The increased mortality due to direct wind damage will cause the dune to become less vegetated and more active until the vegetation cover decreases significantly below the critical vegetation cover, at which point the mortality rate, due to sand drift, increases significantly (as the sand drift is significantly larger than its optimal value). This enhanced mortality will further reduce the psammophilous plant cover and result in an active, almost bare, dune. In order to allow for the psammophilous plant cover to be significant, the wind power has to decrease (or the precipitation rate has to increase) enough to enable $v_p \sim v_c$ and, hence, the sand drift that is optimal for the psammophilous plants. This will result in a bistability of partially covered and bare dunes.

In addition, there is also a bistability of vegetated and partially covered dunes. Starting from a dune partially covered by psammophilous plants, it is possible to decrease their cover by decreasing the wind power. The increased psammophilous plant mortality, due to the reduced sand drift, is accompanied by the decreased mortality of regular vegetation. The enhanced growth of regular vegetation will eventually lead to vegetation cover that is much larger than the critical cover and, therefore, to weak sand drift increasing the regular vegetation cover and decreasing the psammophilous plant cover. In order for the vegetated dune to become only partially covered (involving a transition from a state at which the regular vegetation dominates the cover to a state at which the psammophilous plants dominate the cover), the wind power must increase significantly, such that the mortality rate due to direct wind is large enough to decrease the regular vegetation cover far below the critical value, thereby allowing the psammophilous plants to maintain a cover fraction corresponding to their optimal growth conditions. When the two bistability regions of the psammophilous plants overlap, we find the tristability.

While there are examples for the coexistence of active and fixed dunes under similar climate conditions [*Yizhaq et al.*, 2007, 2009], we are not aware of observations that may be associated with the "new" dune state predicted by model I of moderate cover in which the vegetation cover is close to the critical vegetation cover, v_c (it is important to note that according to this model, the basin of attraction of this state is very small, and therefore, it may not be easily realized in observations). Identifying such a state in observations will provide strong support for the model's setup. We hope to explore this and other features of the model in the future.

The different spatial and temporal scales captured by mean field models and spatially explicit (resolving dune morphology) models make it difficult to compare the results of the two approaches. A significant difference is the fact that in our model, the psammophilous plants are assumed to be affected by the sand drift (including both erosion and deposition) rather than by the sand flux gradient. To the best of our knowledge, most field studies have shown that only a combination of erosion and deposition (sand drift) can enhance the growth rate of psammophilous plants. The different scales, mechanisms, and results of the two modeling approaches call for further field studies at all scales in order to allow better modeling of the effects of psammophilous plants on dune dynamics. It is important to note that the multistability reported here and in previous studies of mean field models has not been reported for models resolving dune morphology.

The model proposed here does not aim to be operative. It aims to provide a qualitative understanding of the dynamics of psammophilous plants in the presence of regular vegetation and BSC. Nevertheless, a comparison with observations of the bistability of sand dunes, reported in *Yizhaq et al.* [2007, 2009], indicates that model I fits the observations better than model II; model II exhibits only an active dune state for drift potential values that are larger than 700 (see Figure 1), while stable dunes exist in nature for higher values of D_p. Model II can to be tuned to fit these observations by increasing $\alpha\_\max_v$ or decreasing ϵ_v. We do not present these results here, in order to use the same parameters in models I and II wherever possible. Another observation that is worth noting concerns the fraction of BSC cover. Both models I and II resulted in BSC cover that does not exceed 25%. Studies have reported almost complete BSC cover on sand dunes for small (order of meters) plots (e.g., Figures 5B and 7 of *Veste et al.* [2011]). This discrepancy between the model and observations can be attributed to the mean field nature of the model, representing only scales of kilometers that usually contain several types of dune surface covers.

The separation of the two growth mechanisms—by assuming optimal growth conditions under either (i) an optimal sand drift or (ii) an optimal wind drift potential—helps us to understand the effect of each of these mechanisms. A more realistic model should include a combination of these two mechanisms, resulting in, most probably, a richer dynamics and steady state map. Observations regarding psammophilous plants may help to determine the role of each mechanism and whether a combination of the two is plausible.

For the parameters used here, model I predicts that the psammophilous plant cover can reach the critical value for sand drift shading, while model II predicts that their fraction of cover is very small. According to each model, there are climate conditions under which the steady state picture is not affected by psammophilous plant cover as an additional dynamical variable in the model. For example, under a low wind drift potential and a high precipitation rate, regular vegetation is the dominant cover type, and the BSC and the psammophilous plants may be ignored. Under extremely dry conditions, $p < 50$ mm/year, and a low wind drift potential, the BSC will be the dominant cover type, and both regular vegetation and psammophilous plants may be ignored. Under an extremely high wind drift potential, the dunes will be fully active without any surface cover. Psammophilous plants may be the dominant cover type under a sufficiently high precipitation rate ($p > 50$ mm/year) and a strong wind drift potential (the definition of strong depends on the model (I or II) and the parameters).

While some of the cover types can be ignored in the steady state, they can still greatly influence the dynamics leading to a steady state. In accordance with the common view [*Danin*, 1996; *Li et al.*, 1992, 1997; *Zhang et al.*, 2005; *Maun*, 2009], we showed that the model predicts that starting from a bare dune state, psammophilous plants may be the first to grow, reducing the sand drift and thus enabling the growth of regular vegetation, which eventually dominates and stabilizes the dunes. This, however, is not always the case as our model predicts that under different climate conditions (wind drift potential), the regular vegetation and psammophilous plants grow equally at first, cooperating in reducing the sand drift, followed by a faster growth of the regular vegetation, which eventually dominates and stabilizes the dunes.

Our preliminary numerical results suggest the possibility of a Hopf bifurcation leading to the oscillatory behavior of the different cover types. This behavior and its relevance to observations, as well as the incorporation of spatial effects in the model, as was done in *Yizhaq et al.* [2013], are left for future research. In addition, we plan to use this model and its extensions to study the response of sand dunes to different scenarios of climate change. We believe that the results of this model, including the complex dynamics and the tristability, may be relevant for many other models of population dynamics.

Acknowledgments
The research leading to these results has received funding from the European Union Seventh Framework Programme (FP7/2007-2013) under grant 293825. This research was also supported by the Israel Science Foundation. We thank Dotan Perlstein for his contribution during the first stages of this research and Shai Kinast for helpful discussions.

References

Anderson, R. S. (1987), A theoretical model for impact ripples, *Sedimentology*, *34*, 943–956, doi:10.1111/j.1365-3091.1987.tb00814.x.
Anderson, R. S., and P. K. Haff (1988), Simulation of eolian saltation, *Science*, *241*(4867), 820–823, doi:10.1126/science.241.4867.820.
Andreotti, B., P. Claudin, and S. Douady (2002), Selection of dune shapes and velocities. Part 2: A two-dimensional modelling, *Eur. Phys. J.*, *28*, 341–352, doi:10.1140/epjb/e2002-00237-3.
Ashkenazy, Y., H. Yizhaq, and H. Tsoar (2012), Sand dune mobility under climate change in the Kalahari and Australian deserts, *Clim. Change*, *112*, 901–923, doi:10.1007/s10,584-011-0264-9.
Baas, A. C. W., and J. M. Nield (2010), Ecogeomorphic state variables and phase-space construction for quantifying the evolution of vegetated aeolian landscapes, *Earth Surf. Processes Landforms*, *35*, 717–731, doi:10.1002/esp.1990.
Bagnold, R. A. (1941), *The Physics of Blown Sand and Desert Dunes*, Chapmann and Hall, London, doi:10.1007/978-94-009-5682-7.
Baudena, M., G. Boni, L. Ferraris, J. von Hardenberg, and A. Provenzale (2007), Vegetation response to rainfall intermittency in drylands: Results from a simple ecohydrological box model, *Adv. Water Res.*, *30*, 1320–1328, doi:10.1016/j.advwatres.2006.11.006.
Charney, J. G., P. H. Stone, and W. J. Quirk (1975), Drought in the Sahara: A biogeophysical feedback mechanism, *Science*, *187*, 434–435, doi:10.1126/science.187.4175.434.
Cheplick, G. P., and K. Grandstaff (1997), Effects of sand burial on purple sandgrass (Triplasis purpurea): The significance of seed heteromorphism, *Plant Ecolog.*, *133*, 79–89, doi:10.1023/A:1009733128430.
Danin, A. (1991), Plant adaptations in desert dunes, *J. Arid Environ.*, *21*, 193–212.
Danin, A. (1996), *Plants of Desert Dunes*, Springer, Berlin.
Danin, A., Y. Bar-Or, I. Dor, and T. Yisraeli (1989), The role of cyanobacteria in stabilization of sand dunes in southern Israel, *Ecol. Mediterr.*, *15*, 55–64.
de M. Luna, M. C. M., E. J. R. Parteli, O. Durán, and H. J. Herrmann (2009), Modeling transverse dunes with vegetation, *Physica A*, *388*, 4205–4217, doi:10.1016/j.physa.2009.06.006.
Durán, O., and H. J. Herrmann (2006), Vegetation against dune mobility, *Phys. Rev. Lett.*, *97*, 188,001, doi:10.1103/PhysRevLett.97.188001.
Eastwood, E., J. Nield, A. Baas, and G. Kocurek (2011), Modelling controls on aeolian dune-field pattern evolution, *Sedimentology*, *58*, 1391–1406, doi:10.1111/j.1365-3091.2010.01216.x.
Forrest, S. B., and P. K. Haff (1992), Mechanics of wind ripple stratigraphy, *Science*, *255*(5049), 1240–1243, doi:10.1126/science.255.5049.1240.
Frederiksen, L., J. Kollmann, P. Vestergaard, and H. H. Bruun (2006), A multivariate approach to plant community distribution in the coastal dune zonation of NW Denmark, *Phytocoenologia*, *36*, 321–342, doi:10.1127/0340-269X/2006/0036-0321.
Fryberger, S. G., and G. Dean (1979), Dune forms and wind regime, in *A Study of Global Sand Seas*, vol. 1052, edited by E. D. McKee, pp. 137–169, U.S. Geol. Surv.
Fryrear, D. W., and J. D. Downes (1975), Estimating seedling survival from wind erosion parameters, *Trans. ASAE*, *18*, 888–891.
Gares, K. F., and P. A. Nordstrom (1995), A cyclic model of foredune blowout evolution for a leeward coast: Island Beach, New Jersey, *Ann. Assoc. Am. Geogr.*, *85*(1), 1–20, doi:10.1111/j.1467-8306.1995.tb01792.x.
Kinast, S., E. Meron, H. Yizhaq, and Y. Ashkenazy (2013), Biogenic crust dynamics on sand dunes, *Phys. Rev. E*, *87*, 020701(R), doi:10.1103/PhysRevE.87.020701.
Kok, J. F., E. J. R. Parteli, T. I. Michaels, and D. B. Karam (2012), The physics of wind-blown sand and dust, *Rep. Prog. Phys.*, *75*, 106901, doi:10.1088/0034-4885/75/10/106901.
Landry, W. L., and B. T. Werner (1994), Computer simulations of self-organized wind ripple patterns, *Physica D*, *77*, 238–260, doi:10.1016/0167-2789(94)90137-6.
Lee, B. E., and B. F. Soliman (1977), An investigation of the forces on three dimensional bluff bodies in rough wall turbulent boundary layers, *Trans. ASME J. Fluid Eng.*, *99*(3), 503–510, doi:10.1115/1.3448828.
Li, S. G., X. L. Chang, and X. Y. Zhao (1992), Researches on Agriophyllum squarrosum the pioneer plant on mobile sand dunes, *J. Arid Reg. Environ. Res.*, *6*, 63–70.
Li, S. G., A. F. Zhao, and X. L. Chang (1997), Several problems about vegetation succession of Horqin Sandy Land, *J. Desert Res.*, *17*, 25–32.
Moreno-Casasola, P. (1986), Sand movement as a factor in the distribution of plant communities in a coastal dune system, *Vegetation*, *65*, 67–76, doi:10.1007/BF00044876.
Martínez, M. L., and P. Moreno-Casasola (1996), Effects of burial by sand on seedling growth and survival in six tropical sand dune species from the Gulf of Mexico, *J. Coast. Res.*, *12*, 406–419.
Martínez, M. L., G. Vázquez, C. S. Sánchez, and S. Colón (2001), Spatial and temporal variability during primary succession on tropical coastal sand dunes, *J. Veg. Sci.*, *12*, 361–372, doi:10.2307/3236850.
Maun, M. A. (1998), Adaptations of plants to burial in coastal sand dunes, *Can. J. Bot.*, *76*, 713–738, doi:10.1139/b98-058.
Maun, M. A. (2009), *The Biology of Coastal Sand Dunes*, Oxford Univ. Press, Oxford, U. K.
Nield, J. M., and A. C. W. Baas (2008), Investigating parabolic and nebkha dune formation using a cellular automaton modelling approach, *Earth Planet. Sci. Lett.*, *33*(5), 724–740, doi:10.1002/esp.1571.
Otterman, J. (1974), Baring high-albedo soils by overgrazing: A hypothesized desertification mechanism, *Science*, *186*, 531–533.
Perumal, V. J., and M. A. Maun (2006), Ecophysiological response of dune species to experimental burial under field and controlled conditions, *Plant Ecolog.*, *184*, 89–104, doi:10.1007/s11258-005-9054-7.
Prigozhin, L. (1999), Nonlinear dynamics of Aeolian sand ripples, *Phys. Rev. E*, *60*(1), 729–733, doi:10.1103/PhysRevE.60.729.
Pye, K. (1982), Morphological development of coastal dunes in a humid tropical environment, Cape Bedford and Cape Flattery, North Queensland, *Geogr. Ann.*, *64*, 213–227, doi:10.2307/520647.
Pye, K., and H. Tsoar (1990), *Aeolian Sand and Sand Dunes*, Unwin Hyman, London, doi:10.1007/978-3-540-85910-9.
Reitz, M. D., D. J. Jerolmack, R. C. Ewing, and R. L. Martin (2010), Barchan-parabolic dune pattern transition from vegetation stability threshold, *Geophys. Res. Lett.*, *37*, L19402, doi:10.1029/2010GL044957.
Shanas, U., et al. (2006), Reptile diversity and rodent community structure across a political border, *Biol. Conserv.*, *132*, 292–299, doi:10.1016/j.biocon.2006.04.021.
Thomas, D. S. G., and G. F. S. Wiggs (2008), Aeolian systems response to global change: Challenges of scale, process and temporal integration, *Earth Surf. Processes Landforms*, *33*(9), 1396–141, doi:10.1002/esp.1719.
Thomas, D. S. G., M. Knight, and G. F. S. Wiggs (2005), Remobilization of southern African desert dune systems by twenty-first century global warming, *Nature*, *435*, 1218–1221, doi:10.1038/nature03717.
Tsoar, H. (2005), Sand dunes mobility and stability in relation to climate, *Physica A*, *357*(1), 50–56, doi:10.1016/j.physa.2005.05.067.
Tsoar, H. (2008), Land use and its effect on the mobilization and stabilization of the NW Negev sand dunes, in *Arid Dune Ecosystems, Ecological Studies*, vol. 200, edited by S. W. Breckle, A. Yair, and M. Veste, pp. 79–90, Springer, Berlin, doi:10.1007/978-3-540-75498-5_6.

Veste, M., T. Littman, S.-W. Breckle, and A. Yair (2001), The role of biological soil crusts on desert sand dunes in the northwestern Negev, Israel, in *Sustainable Land Use in Deserts*, edited by S.-W. Breckle, M. Veste, and W. Wucherer, pp. 357–367, Springer, Berlin Heidelberg, doi:10.1007/978-3-642-59560-8_38.

Veste, M., K. Breckle, S. W. Eggert, and T. Littmann (2011), Vegetation pattern in arid sand dunes controlled by biological soil crusts along a climatic gradient in the Northern Negev desert, *Basic Appl. Dryland Res.*, *5*, 1–17.

Wagner, R. H. (1964), The ecology of Uniola paniculata L. in the dune-strand habitat of North Carolina, *Ecol. Monogr.*, *34*, 79–96, doi:10.2307/1948464.

Wallen, B. (1980), Changes in structure and function of Ammophila during primary succession, *Oikos*, *34*, 227–238.

Wolfe, S. A., and W. C. Nickling (1993), The protective role of sparse vegetation in wind erosion, *Prog. Phys. Geog.*, *17*, 50–68, doi:10.1177/030913339301700104.

Yizhaq, H. (2005), A mathematical model for aeolian megaripples on Mars, *Physica A*, *357*, 57–63, doi:10.1016/j.physa.2005.05.070.

Yizhaq, H. (2008), Aeolian megaripples: Mathematical model and numerical simulations, *J. Coastal Res.*, *24*(6), 1369–1378, doi:10.2112/08A-0012.1.

Yizhaq, H., Y. Ashkenazy, and H. Tsoar (2007), Why do active and stabilized dunes coexist under the same climatic conditions? *Phys. Rev. Lett.*, *98*, 188001, doi:10.1103/PhysRevLett.98.188001.

Yizhaq, H., Y. Ashkenazy, and H. Tsoar (2009), Sand dune dynamics and climate change: A modeling approach, *J. Geophys. Res.*, *114*, F01023, doi:10.1029/2008JF001138.

Yizhaq, H., Y. Ashkenazy, N. Levin, and H. Tsoar (2013), Spatiotemporal model for the progression of transgressive dunes, *Physica A*, *392*(19), 4502–4515, doi:10.1016/j.physa.2013.03.066.

Zhang, J., and M. A. Maun (1990), Effects of sand burial on seed germination, seedling emergence, survival, and growth of Agropyron psammophilum, *Can. J. Bot.*, *68*, 304–310, doi:10.1139/b90-041.

Zhang, J., and M. A. Maun (1992), Effects of burial in sand on the growth and reproduction of Cakile edentula, *Ecography*, *15*, 296–302, doi:10.1111/j.1600-0587.1992.tb00038.x.

Zhang, J., H. Zhao, T. Zhang, X. Zhao, and S. Drake (2005), Community succession along a chronosequence of vegetation restoration on sand dunes in Horqin Sandy Land, *J. Arid Environ.*, *62*, 555–566, doi:10.1016/j.jaridenv.2005.01.016.